WILEY VCH

RESEARCH ARTICLE

# $I_3^-$-mediated oxygen evolution activities to boost rechargeable zinc-air batteries with low charging voltage and long cycling life

Xiaohong Zou, Qian Lu, Lizhen Wu, Kouer Zhang, Mingcong Tang, Haijiao Xie, Xiao Zhang*, Zongping Shao*, Liang An*

[a] Dr. X. Zou, Mr. L. Wu, Ms. K. Zhang, Mr. M. Tang, Prof. X. Zhang, Prof. L. An
Department of Mechanical Engineering, The Hong Kong Polytechnic University, Hung Hom, Kowloon, Hong Kong SAR, PR China
E-mail: liang.an@polyu.edu.hk; xiao1.zhang@polyu.edu.hk

[b] Dr. Q. Lu
Jiangsu Collaborative Innovation Center of Atmospheric Environment and Equipment Technology, Jiangsu Key Laboratory of Atmospheric Environment Monitoring and Pollution Control, School of Environmental Science and Technology, Nanjing University of Information Science and Technology, Nanjing 210044, PR China

[c] Dr. Q. Lu
Department of Chemistry, The Chinese University of Hong Kong, Ma Lin building, Shatin 999077, Hong Kong SAR, PR China

[d] Ms. H. Xie
Hangzhou Yanqu Information Technology Co., Ltd. Y2 2 nd Floor, Building 2, Xixi Legu Creative Pioneering Park, No. 712 Wen'er West Road, Xihu District, Hangzhou City, Zhejiang Province, 310003, P.R.O.C.

[e] Prof. Z. Shao
WA School of Mines: Minerals, Energy and Chemical Engineering (WASM-MECE), Curtin University, Perth, WA 6102, Australia
E-mail: zongping.shao@curtin.edu.au

[f] Prof. X. Zhang, Prof. L. An
Research Institute for Advanced Manufacturing, The Hong Kong Polytechnic University, Hung Hom, Kowloon, Hong Kong SAR, PR China

[g] Prof. X. Zhang, Prof. L. An
Research Institute for Smart Energy, The Hong Kong Polytechnic University, Hung Hom, Kowloon, Hong Kong SAR, PR China

Supporting information for this article is given via a link at the end of the document.

**Abstract:** An effective strategy to facilitate oxygen redox chemistry in metal-air batteries is to introduce a redox mediator into the liquid electrolyte. The rational utilization of redox mediators to accelerate the charging kinetics while ensuring the long lifetime of alkaline Zn-air batteries is challenging. Here, we apply commercial acetylene black catalysts to achieve an $I_3^-$-mediated Zn-air battery by using $ZnI_2$ additives that provide $I_3^-$ to accelerate the cathodic redox chemistry and regulate the uniform deposition of $Zn^{2+}$ on the anode. The Zn-air battery performs an ultra-long cycle life of over 600 h at 5 mA $cm^{-2}$ with a final charge voltage of 1.87 V. We demonstrate that $I^-$ mainly generates $I_3^-$ on the surface of carbon catalysts during the electrochemically charging process, which can further chemically react with $OH^-$ to generate oxygen and further revert to $I^-$, thus obtaining a stable electrochemical system. This work offers a strategy to simultaneously improve the cycling life and reduce the charging voltage of Zn-air batteries through redox mediator methods.

## Introduction

Searching for high-efficiency energy storage/conversion systems is an urgent priority to reduce $CO_2$ emissions to achieve carbon neutrality [1]. Zn-air batteries have aroused great concern due to their high theoretical energy density and environmental friendliness [2]. Unfortunately, Zn-air batteries still suffer from high charging voltages, generally higher than 1.9 V, offering a lower energy efficiency [3]. Specifically, the high charging voltages in the Zn-air battery system would induce the corrosion and dissolution of catalysts under a high oxidation state, finally causing fast decay of cyclic performance[4]. Although many catalysts for oxygen evolution reaction (OER) have been developed to reduce the charging voltage of Zn-air batteries, the results obtained so far are unsatisfactory.

Introducing redox mediators into the liquid electrolyte has been proven to be an effective strategy for $O_2$ redox chemistry in metal-air batteries, such as Li-$O_2$ batteries, Zn-air batteries, and Al-air batteries [5]. The reaction pathway of the Zn-air battery could be changed to a more active state for accelerating charge kinetics and lowering the oxidation voltage when adding redox mediators with a lower electrochemical potential than the oxidation potential of $OH^-$ to $O_2$ [6]. For instance, Wang et al. found that the soluble catalyst anthraquinone-2, 7-disulfonic acid disodium salt (AQDS) could effectively boost the discharge performance of Zn-air batteries by completing the two-electron oxygen redox chemistry [7]. The soluble redox mediator could extend the active area due to the redox reaction occurring in the electrolyte. For oxygen reduction reaction (ORR), it is necessary to construct an effective three-phase interface for oxygen accessibility. Therefore, the improvement of discharge performance by redox mediator is limited, which is extremely effective for the charging process.

Moreover, the solid-state Zn-air batteries demonstrate their great potential in flexible and wearable devices, therefore, the designed flexible Zn-air battery with reduced charging voltage even under different bending conditions will highlight its potential in practical devices[8] .

Current research indicates that $I_3^-/I^-$ is a reasonable redox mediator to regulate the redox chemistry of metal-air batteries [9]. Huang et al. introduced an $I_3^-/I^-$ redox mediator into organic Zn-air batteries to accelerate the electrooxidation of $Zn_5(OH)_8Cl_2{\cdot}H_2O$ by $I_3^-$ during the charging process and regulate the energy level of ORR by adsorbed $I^-$ on catalysts during the discharging process. However, the organic system involves the decomposition of solid products and two-phase interfaces at the air cathode, resulting in a low current density of only 0.4 mA $cm^{-2}$ [10]. To address this point, Ni et al. proposed adding soluble potassium iodide into an alkaline electrolyte to change the charging reaction from the OER pathway to $I^-$ oxidation reaction (IOR) by using Pt/C catalysts [11]. Although a low charging potential is obtained, the whole Zn-air battery is not a stable system because IOR keeps consuming $I^-$ to produce $IO_3^-$, resulting in a low lifetime of 80 h at 5 mA $cm^{-2}$. To avoid the production of $IO_3^-$, we believe that anodic catalysts must have a weak $I^-$ oxidation capacity to produce $I_3^-$ redox mediators. Rational utilization of $I_3^-/I^-$ redox mediators to accelerate the charging kinetics while ensuring the long lifetime of alkaline rechargeable aqueous and solid-state Zn-air batteries is challenging.

Here we select commercial carbon catalysts to achieve an $I_3^-$-mediated Zn-air battery by using $ZnI_2$ additive, which provides $I_3^-$ to accelerate the cathodic redox chemistry and regulates the uniform deposition of $Zn^{2+}$ on the anode. The Zn-air battery with carbon catalysts and 0.2 M $ZnI_2$ additive achieves an ultra-long cycle life of over 600 h at 5 mA $cm^{-2}$ with a final charge voltage of 1.87 V. In addition, the solid-state Zn-air battery with $ZnI_2$ additive could operate stably for over 1500 min without any voltage decay. Based on electrochemical tests, *in situ* spectroscopy, and energy spectra, we demonstrate that $I^-$ mainly generates $I_3^-$ on the surface of carbon catalysts during the charging process, which can chemically react with $OH^-$ to generate oxygen and further restore to $I^-$. We believe that the concept of $I_3^-$-mediated aqueous Zn-air batteries can guide further research to simultaneously reduce the charge voltage and improve cycle life in the future, and provide new insight into designing soluble catalysts for highly efficient rechargeable Zn-air batteries.

## Results and Discussion

We select zinc iodide ($ZnI_2$) as an additive for Zn-air batteries instead of conventional zinc salts to explore $I_3^-/I^-$ used as a redox mediator, for reducing the overpotential. To avoid excessive oxidation of $I^-$, we chose commercial acetylene black carbon with abundant oxygen species as the air electrode catalyst for exploration (Figure S1) [12]. The cycling performance of Zn-air batteries with different $ZnI_2$ concentrations was first evaluated in Figure 1a. When the concentration of $ZnI_2$ was increased to 0.2 M, the cycle life of the Zn-air battery increased significantly, while the cycle life of the Zn-air battery decreased as the concentration of $ZnI_2$ continued to increase. This phenomenon is different from the conventional $I^-$ oxidation reaction (IOR), where the reaction time increases with the concentration of $I^-$ reactant. The corrosive effect of $IO_3^-$ on the carbon catalyst during the charging process is the main reason for the reduction in cycle life at high $I^-$ concentrations (Figure S2). The high charging voltage in low $ZnI_2$ concentration can also reduce the cycling performance, therefore, there exists an optimal $ZnI_2$ concentration that can simultaneously maintain a low charging potential and a long cycle life. In addition, Figure 1b compares the charging voltage of Zn-air batteries at different $ZnI_2$ concentrations and shows that the charging voltage decreases with increasing $ZnI_2$ concentration, indicating a gradual increase in the participation of $I^-$ oxidized to $IO_3^-$ considering the low potential of $IO_3^-/I^-$ than $I_3^-/I^-$. At $ZnI_2$ concentrations above 0.3 M, the initial charging voltage of Zn-air batteries showed a significant polarization potential, which is attributed to the fact that $I^-$ is first oxidized to $I_3^-$ at a high potential ($E^\theta$ = 0.53 V vs. SHE) and then $I_3^-$ continues to be oxidized to $IO_3^-$ at a low potential ($E^\theta$ = 0.26 V vs. SHE). As shown in Figure 1c, the initial charging voltage decreases with increasing the concentration of $ZnI_2$, When the concentration of $ZnI_2$ is higher than 0.3 M, the initial charging voltage decreases more significantly, while the charging potential remains unchanged when $ZnI_2$ concentration is higher than 0.5 M. In addition, the relationship between cycling life and $ZnI_2$ concentration in electrolytes follows a volcanic trend. Therefore, as the concentration of $ZnI_2$ increases, the charging reaction on the carbon catalyst shifts from $I_3^-/I^-$ at low concentrations to $IO_3^-/I^-$ at high concentrations considering the corrosive effect of $IO_3^-$ on carbon catalysts and the volcanic trend of cycling life.

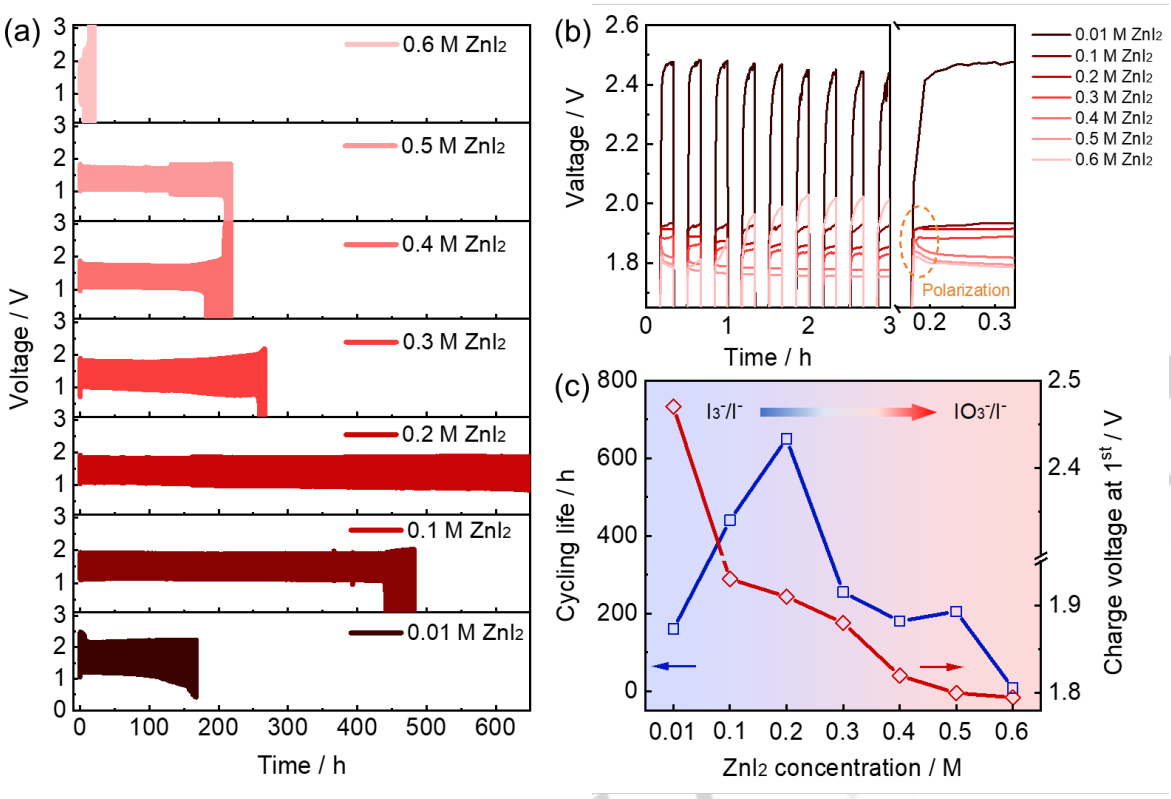


**Figure 1.** (a) Galvanostatic curve of Zn-air batteries with adding different $ZnI_2$ concentrations. (b) Initial charging curve of Zn-air batteries with adding different $ZnI_2$ concentrations. (c) Cycling life and an initial charging voltage of Zn-air batteries with adding different $ZnI_2$ concentrations. Test current density: 5 mA $cm^{-2}$.

In IOR-dominated Zn-air batteries, although a low charging potential can be achieved, $I^-$ is oxidized to $IO_3^-$ during the cycles, and high $IO_3^-$ concentration is also detrimental to the stability of air catalysts, resulting in poor stability. In contrast, in the case of $I_3^-$-mediated OER, the $I_3^-/I^-$ redox reaction does not affect the $I^-$ concentration, while $I_3^-$ can also facilitate the OER kinetic to reduce charging voltage as illustrated in Figure 2a. $I^-/I_3^-$ redox reactions can be achieved on carbon catalysts (Figure S3). Therefore, we chose an alkaline electrolyte with a concentration of 0.1 M $I^-$ to further investigate the $I_3^-/I^-$ redox reaction on carbon catalysts in a three-electrode cell (Figure S4). For comparison, commercial Pt/C and $RuO_2$, serving as ORR and OER catalysts, were also considered. The standard potential of $I_3^-/I^-$ and $IO_3^-/I^-$ redox reactions are 0.53 and 0.26 V, respectively, which indicates that the equilibrium potential of $I_3^-/I^-$ and $IO_3^-/I^-$ redox reactions are 1.36 and 1.09 V, respectively. As shown in Figure 2b, we can observe the $I_3^-/I^-$ redox reactions carried out on carbon catalysts from the cyclic voltammetry (CV) curves, while the area of reduction peak for $I_3^-$ to $I^-$ was greatly reduced for Pt/C and $RuO_2$, which demonstrates the irreversible $I^-$-oxidation reaction owning to the production of $IO_3^-$. The redox peak above 1.75 V can be attributed to the over-oxidation of $I_3^-$ species (Figure S3) [13]. In the reduction region, a CV peak attributed to oxygen reduction reaction (ORR) can be observed for both carbon, Pt/C, and $RuO_2$ catalysts in Figure 2c. Moreover, for $RuO_2$ and Pt/C catalysts, a distinct reduction CV peak of $IO_3^-$ to $I^-$ can be observed near 0.35 V vs. RHE, while no $IO_3^-$ reducing peaks were observed for carbon catalysts (Figure S5), which further proves the well $I_3^-/I^-$ redox reaction on carbon catalysts. The ORR potential in alkaline electrolyte with 0.1 M KI was also higher than that in alkaline electrolyte in Figure 2d.

We further evaluate the OER activity of carbon catalysts in 0.1 M KOH with 0.1 M KI electrolyte in Figure 2e. It can be seen that there are two reaction regions corresponding to IOR at low potential and $I_3^-$-mediated OER at high potential for $RuO_2$ and Pt/C, whereas only $I_3^-$-mediated OER after 1.4 V vs. RHE occurs on carbon catalysts. The $I_3^-$-mediated OER activity of carbon catalyst at high current density is even better than that of Pt/C and $RuO_2$ owing to the competition between IOR and $I_3^-$-mediated OER on Pt/C and $RuO_2$ catalysts. Carbon catalysts delivered almost no OER activity in 0.1 M KOH while offering a low OER potential of 1.45 V at 10 mA $cm^{-2}$ in 0.1 M KOH with 0.1 M KI, which is also better than commercial $IrO_2$ in 0.1 M KOH (Figure S6a-c). In addition, we also compare our work with recently reported Ru-based, NiFe-based, and complex oxide-based catalysts (Figure S6d and Table S1), revealing the superiority of our work. The $I_3^-$-mediated OER stability of carbon catalysts in 0.1 M KOH with 0.1 M KI electrolyte was further evaluated in Figure S7. Carbon catalysts can be stably operated at 10 mA $cm^{-2}$ for more than 40 h without potential degradation, suggesting that $I_3^-$-mediated OER on carbon catalysts is a stable system without occurring IOR to consume $I^-$.

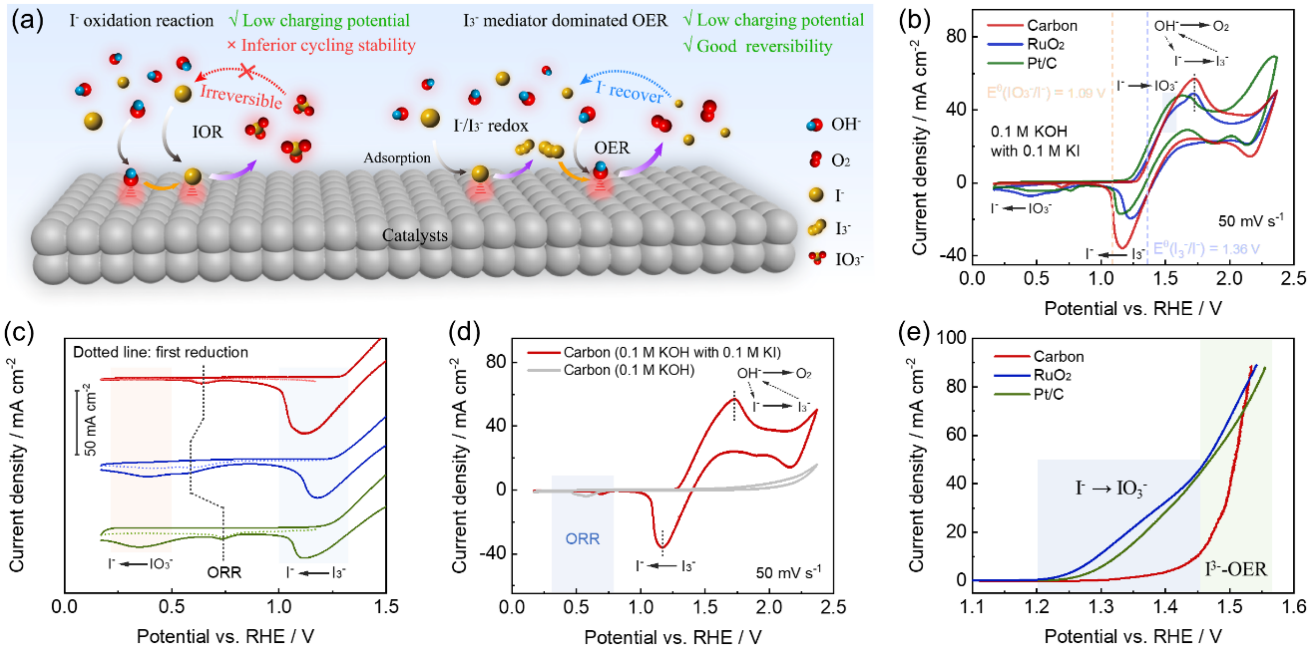


**Figure 2.** (a) The schematic diagram of $I^-$ oxidation reaction and $I_3^-$ mediator dominated OER. (b, c) Cyclic voltammetry curve of different catalysts in $O_2$-saturated 0.1 M KOH with 0.1 M KI under a scan rate of 50 mV $s^{-1}$. (d) CV curve of carbon catalysts in $O_2$-saturated 0.1 M KOH with or without 0.1 M KI under a scan rate of 50 mV $s^{-1}$. (e) LSV polarization curve of carbon catalyst in $O_2$-saturated 0.1 M KOH with 0.1 M KI. Rotation speed: 1600 r.p.m., Scan rate: 10 mV $s^{-1}$.

The electrochemical results indicate that $I_3^-$-mediated OER mainly occurred on carbon catalysts. To reveal the reaction mechanism, we further applied *in situ* UV-Vis technology to detect the $I_3^-$ concentration on carbon cathode in Zn-air batteries during the charge/discharge process as shown in Figure 3a. The characteristic peaks of around 348 nm associated with $I_3^-$ delivered the increased intensity with increasing charging time (Figure 3b) [14], while the characteristic peak quickly disappeared after the discharging process due to the rapid consumption of $I_3^-$ by $OH^-$ to produce $O_2$ (Figure S8), which indicates that the charging and discharging process is accompanied by $I_3^-/I^-$ redox reaction. To exclude the effect of over-oxidation to $IO_3^-$, we further tested the composition of electrolytes after the 40 h OER test (Electrode area: 1 × 1 $cm^2$) through X-ray photoelectron spectrometers (XPS). As shown in Figure 3c, only two peaks, I $3d_{3/2}$ and I $3d_{5/2}$, attributed to $I^-$, were observed at 630.2 and 618.6 eV, respectively, while I Auger spectra also confirm the presence of only $I^-$ in the electrolyte after OER stability (Figure S9) [15]. Therefore, carbon catalysis hardly over-oxidizes $I^-$ to $IO_3^-$, but oxidizes to $I_3^-$, which acts as a redox mediator to accelerate OER activity.

The carbon catalysts showed poor stability at high $I^-$ concentrations, which we hypothesized was mainly due to the corrosion of carbon catalysts during OER. Further analysis of the surface composition of carbon catalysts before and after the charging test was carried out. After the first charge step in Figure 3d, we can observe four XPS peaks associated with $IO_3^-$ and $I^-$, indicating that the oxygen site in carbon catalysts will be attacked by adsorbed $*I_3^-$ and $OH^-$ during the charging process to generate surface-adsorbed $IO_3^-$ (Figure S10) [16]. In addition, $I_2$ will not be generated on the carbon catalyst during the charging process (Figure S11). After further discharge step, the XPS characteristic peak of $IO_3^-$ still exists, revealing that $IO_3^-$ corrosion of carbon catalysts surface is irreversible, which is also the reason for the poor stability of carbon catalysts under high $I^-$ concentration. Raman spectra of carbon catalysts showed an obvious blue shift of v(O−H) bands for the $H_2O$ molecule after the charging test in an electrolyte containing $I^-$ due to the adsorption of $IO_3^-$ on carbon catalysts, while the binding energy of *OH is not affected (Figure S12), indicating that adsorbed $IO_3^-$ does not affect the adsorption of *OH on carbon catalysts [17]. At a suitable $I^-$ concentration, here is 0.2 M, $IO_3^-$ is tightly adsorbed on the oxygen sites of carbon catalysts without resolving into the electrolyte, thus further corrosion can be avoided.

We further extracted the reaction mechanism from charge/discharge curves. As shown in Figure 3e, the first discharge in 6 M KOH + 0.2 M $ZnI_2$ shows only one voltage plateau corresponding to oxygen reduction reaction (ORR), whereas the second discharge provides two reaction processes, including the reduction of $I_3^-$ and ORR. During the charging step, carbon catalysts first decompose to carbonate, then $I^-$ is electrochemically oxidized to $I_3^-$, which reacts with $OH^-$ to form oxygen and $I^-$. The discharge process shows a small plateau from $I_3^-$ to $I^-$, as most of the $I_3^-$ is converted to $I^-$ during the charging process. In contrast, the first and second discharge of Zn-air batteries in 6 M KOH + 0.2 M $ZnCl_2$ offers one voltage plateau corresponding to ORR (Figure S13). In addition, two obvious corrosion voltage plateaus in the charging curve can be observed for $Cl^-$-containing electrolyte[18]. The low decomposing capacity of carbon in $I^-$-containing electrolyte means $I_3^-$ can restrain the decomposition of carbon catalysts. We also calculate the reaction energy of $I^-$ oxidized to $I_3^-$ through theoretical calculation. The

oxidation of $I^-$ to $I_3^-$ delivers the free energy of 10.31 eV, while the further oxidation of $I_3^-$ to $I_2$ shows the free energy of 10.55 eV (Figure 3f), revealing that $I_3^-$ is the main oxidation product. In addition, the further chemical oxidation of $OH^-$ with $I_3^-$ to $O_2$ and $H_2O$ offers a free energy of -7.73 eV, while the electrochemical oxidation of $OH^-$ to $O_2$ and $H_2O$ shows a free energy of 12.90 eV (Figure 3g), indicating that $I_3^-$ can facilitate the oxidation of $OH^-$ and thus reduce the charging potential of Zn-air batteries. Therefore, we propose a reaction mechanism for $I_3^-$-mediated OER in Figure 3h. During the charging process, $I^-$ is first electrochemically oxidized to $I_3^-$ on carbon catalysts, then $I_3^-$ chemically reacts with $OH^-$ to form $O_2$ and $I^-$. The catalytic system returns to its original state, which is the main reason for the excellent stability in the 0.2 M $ZnCl_2$ electrolyte.

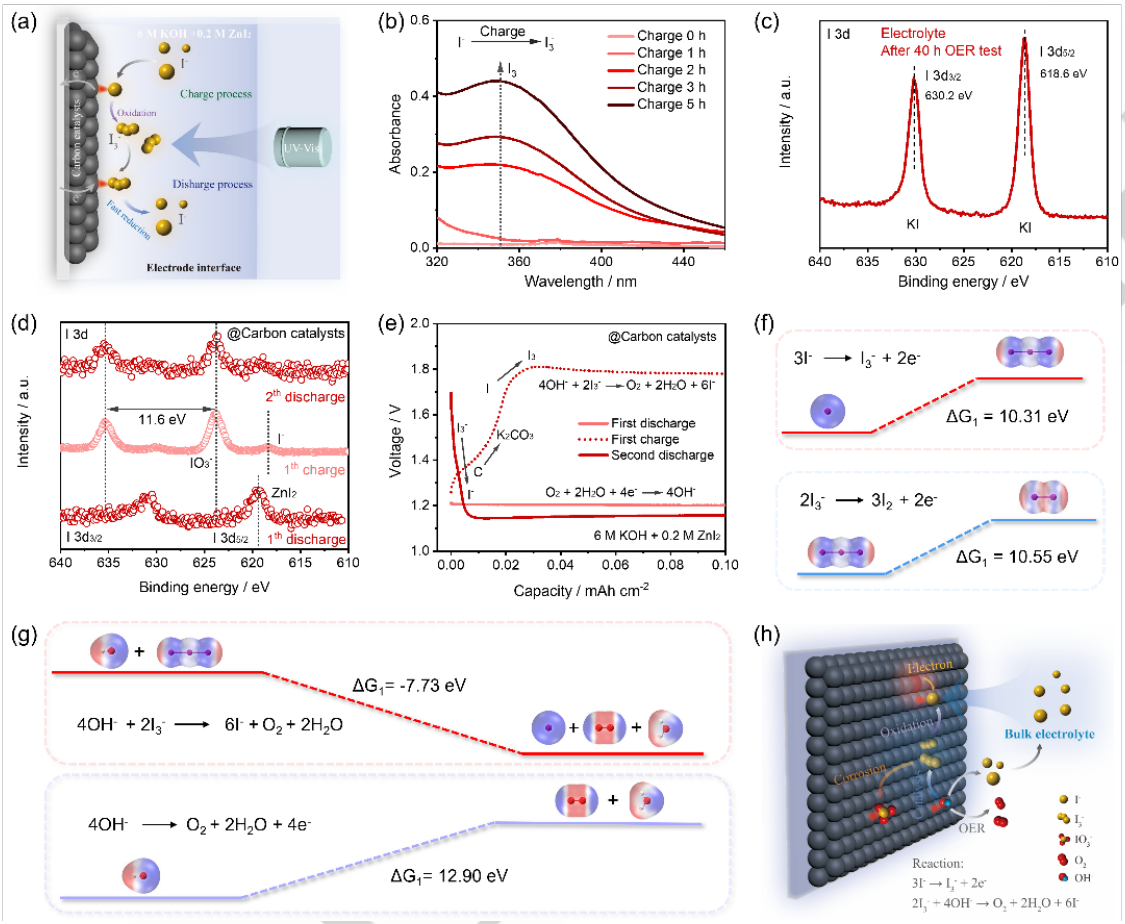


**Figure 3.** (a) The schematic diagram of testing $I_3^-$ concentration on carbon electrode in Zn-air batteries with 6 M KOH + 0.2 M $ZnI_2$ during charge/discharge process by *in situ* UV-Vis technology. (b) UV-Vis spectra during different charge times for Zn-air batteries with 6 M KOH + 0.2 M $ZnI_2$ electrolyte. (c) XPS I 3d spectra of electrolyte after 40 h OER test at 10 mA $cm^{-2}$. (d) XPS I 3d spectra of carbon catalysts after different cycles for Zn-air batteries at 5 mA $cm^{-2}$. (e) Galvanostatic discharge and charge curves of Zn-air batteries with 6 M KOH + 0.2 M $ZnI_2$ electrolyte at 1 mA $cm^{-2}$. (f) The reaction free energy of $I^-$ and $I_3^-$ oxidation. (g) The reaction free energy of $I_3^-$-mediated OER and conventional OER. (h) Reaction mechanism of carbon catalysts for Zn-air batteries with $I_3^-/I^-$ redox mediator.

Generally, zinc salt needs to be added to the alkaline electrolyte to assist in the decomposition of ZnO during the charging process [19]. As shown in Figure S14, the Zn-air battery with KI additives shows high charging voltage at the initial stage. Here we choose $ZnI_2$ as an additive to replace conventional zinc salt additives, such as $ZnCl_2$ and $Zn(Ac)_2$. To confirm that $ZnI_2$ additives can be applied to Zn-based batteries, we further investigate the effect of $ZnI_2$ additives on zinc anode. The $ZnI_2$ additive can restrain the activity of hydrogen evolution reaction on the zinc anode (Figure S15), improve the ion conductivity (Figure S16), enlarge the electrochemical window (Figure S17), and reduce the interfacial resistance for Zn deposition (Figure S18). In addition, Zn||Zn symmetrical cells and Zn||Cu asymmetrical cells with $ZnI_2$ additive offer a better long lifespan and low plating/stripping overpotential (Figure S19 - S24). In electrolytes containing $ZnI_2$, a uniform Zn-I protective layer is formed on the surface of the zinc anode after 100 cycles in Zn-air batteries (Figure S25), thus regulating the uniform deposition of zinc ions (Figure S26). Detailed information can be found in Supplementary Note 1. Therefore, the $I_3^-/I^-$ redox mediator optimizes the deposition of zinc ions, which in combination with the cathode catalytic reaction improves the cycle life of Zn-air batteries.

We finally compare the performance of two electrolytes, 6 M KOH + 0.2 M $ZnI_2$ and 6 M KOH + 0.2 M $ZnCl_2$, in rechargeable Zn-air batteries as shown in Figure 4a. The Zn-air battery with 6 M KOH + 0.2 M $ZnI_2$ offers a high discharge capacity (Figure S27), high power density, and low charging overpotential (Figure S28). Significantly, the Zn-air battery with 6 M KOH + 0.2 M $ZnI_2$ achieves an ultra-long cycle life of over 600 h at 5 mA $cm^{-2}$ with a final charge voltage of 1.87 V, compared to just 2 h for the battery with 6 M KOH + 0.2 M $ZnCl_2$ electrolyte in Figure 4b. We can find that the cycle life of this work far exceeds the reported Zn-air

batteries with KI addictive (Figure 4c and Table S2) and bifunctional catalysts (Table S3), revealing the superiority of our work by combining carbon catalysts with $ZnI_2$ addictive. Moreover, the Zn-air battery with 6 M KOH + 0.2 M $ZnI_2$ can achieve a stable cycle for over 200 hours at 10 mA $cm^{-2}$ (Figure S29). In addition, we also test the rate performance of Zn-air batteries under different current densities (5 - 40 mA $cm^{-2}$) in Figure S30. The Zn-air battery with 6 M KOH + 0.2 M $ZnI_2$ performs no significant increase in voltage as the current density increases and a low charge voltage of 1.9 V at 40 mA $cm^{-2}$. To explore the effect of $ZnI_2$ on oxygen bubble evolution during the charging process, we adopted *in situ* optical observation to record the oxygen bubble evolution of the air cathode at 40 mA $cm^{-2}$ in Figure 4d and S31 [20]. As shown in Figure 4e, we can observe abundant small oxygen bubbles on the cathode surface during the charging test with area capacity of 25 mAh $cm^{-2}$ at 40 mA $cm^{-2}$ while the charge voltage of Zn-air batteries with $ZnI_2$ addictive is just ~2.0 V, confirming that the $ZnI_2$ additive in electrolytes would accelerate the OER kinetics instead of IOR in the Zn-air system. In addition, there are more and smaller bubbles on the surface of carbon electrodes in electrolytes containing $ZnI_2$, which is mainly due to the uniform dispersion of $I_3^-$ redox mediators that react with $OH^-$ to produce oxygen on the carbon catalyst surface.

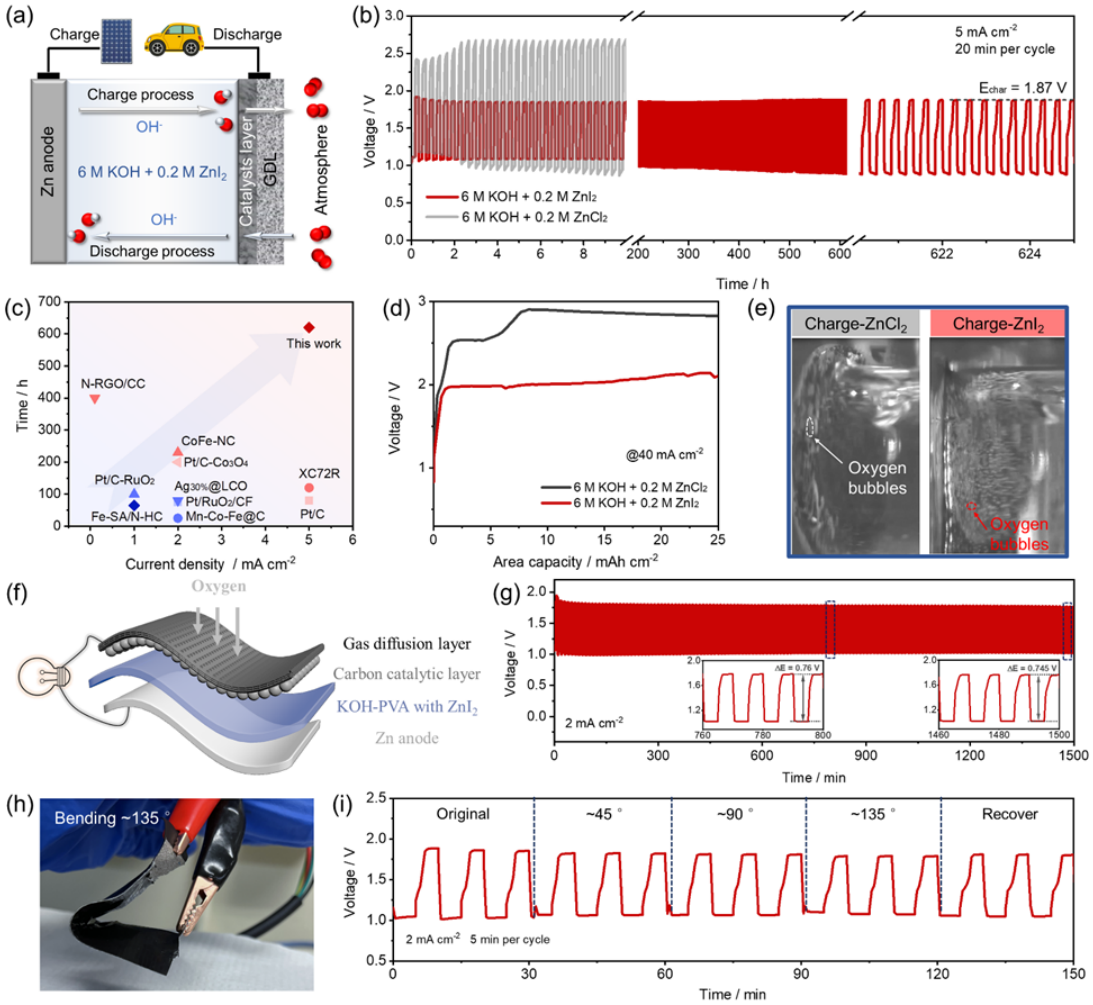


**Figure 4.** (a) The schematic illustration of rechargeable Zn-air batteries. (b) Galvanostatic discharging/charging curve of Zn-air batteries with and without $ZnI_2$ additive at 5 mA $cm^{-2}$. (c) The comparison of cycling life and current density of Zn-air batteries with KI additive. (d) The charging curve of Zn-air batteries at 40 mA $cm^{-2}$ while observing the generation of oxygen bubbles. (e) *In situ* observation of cathode surface for Zn-air batteries with $ZnCl_2$ and $ZnI_2$ additive at 40 mA $cm^{-2}$ during the charging process. (f) Schematic illustration of the flexible Zn-air battery configuration with PVA matrix immersed with 6 M KOH + 0.2 M $ZnI_2$. (g) Galvano-dynamic discharging/charging curves of the flexible Zn-air battery at 2 mA $cm^{-2}$. (h) The image at a bending angle of 135° and (i) Galvano-dynamic charge and discharge polarization curves of flexible Zn-air batteries under various bending conditions.

To highlight the practical application of the concept of $I_3^-/I^-$ redox mediators, we also assemble the solid-state Zn-air battery with carbon catalysts and polyvinyl alcohol (PVA) electrolytes with 6 M KOH + 0.2 M $ZnI_2$ as shown in Figure 4f. The solid-state Zn-air battery with $ZnI_2$ additive could stably cycle for over 1500 min at 2 mA $cm^{-2}$, while there was no attenuation in charging and discharging voltages in Figure 4g, which is also comparable to the currently reported flexible Zn-air batteries (Table S4). In addition, the flexible battery with $ZnI_2$ additive has an open-circuit voltage of 1.29 V, while maintaining a stable open-circuit voltage under various bending conditions (Figure 4h and S32). Once the original condition had been restored, the voltage remained stable at 1.31 V. To further evaluate the flexibility, the charge/discharge performance under various bending conditions was also obtained

in Figure 4i. The solid-state Zn-air battery with $ZnI_2$ additive offers the same discharge/charge voltage under flat and various bending conditions, revealing its excellent flexibility (Figure S33). Based on the above results, we believe that carbon catalysts are an optional option for achieving $I_3^-$-mediated OER. However, the poor ORR activity of carbon catalysts makes them exhibit lower discharge potentials in Zn-air batteries. Therefore, we believe that heteroatom-doped carbon materials can be subsequently designed to improve the discharge performance of $I_3^-$-mediated Zn-air batteries.

## Conclusion

In conclusion, we have successfully applied carbon catalysts to achieve an $I_3^-$-mediated Zn-air battery with an ultra-long cycle life of over 600 h at 5 mA $cm^{-2}$ at a final charge voltage of 1.87 V. The concept of redox mediators could also be extended to solid-state Zn-air batteries. To prove the reaction mechanism of $I_3^-$ on carbon catalysts, we have confirmed through electrochemical tests, *in situ* spectroscopy, and energy spectra that $I^-$ mainly generates $I_3^-$ on the surface of carbon catalysts during the charging process, which can further react with $OH^-$ following a chemical step to generate oxygen and recover to $I^-$. This work presents an available strategy to simultaneously improve the cycle life and reduce the charging voltage of Zn-air batteries through redox mediator strategies, which also guides the subsequent design of efficient carbon catalysts for $I_3^-$-mediated Zn-air batteries.

## Supporting Information

The authors have cited additional references within the Supporting Information.

## Acknowledgements

L. An (Liang An) thanks the grant from the Research Institute for Smart Energy (CDA4), the grant from the Research Institute for Advanced Manufacturing (CD8Z), and the grant from the Carbon Neutrality Funding Scheme (WZ2R) at The Hong Kong Polytechnic University. X. Zhang (Xiao Zhang) acknowledges the support from the Hong Kong Polytechnic University (CD9B, CDBZ and WZ4Q), the National Natural Science Foundation of China (22205187) and Shenzhen Municipal Science and Technology Innovation Commission (R2023A045). Q. Lu (Qian Lu) thanks the Start-up Foundation for Introducing Talent of NUIST and Natural Science Foundation of Jiangsu Province of China (BK20230426).

## Conflict of Interest

The authors declare no conflict of interest.

## Data Availability Statement

The data that support the findings of this study are available from the corresponding author upon reasonable request.

**Keywords:** Zinc-air batteries • Redox mediators • oxygen electrocatalysts • Redox chemistry • Stability

[1] aM. C. Luo, Z. L. Zhao, Y. L. Zhang, Y. J. Sun, Y. Xing, F. Lv, Y. Yang, X. Zhang, S. Hwang, Y. N. Qin, J. Y. Ma, F. Lin, D. Su, G. Lu, S. J. Guo, *Nature* **2019**, *574*, 81; bW. X. Wu, L. P. Xu, Q. Lu, J. P. Sun, Z. Y. Xu, C. S. Song, J. C. Yu, Y. Wang, *Adv. Mater.* **2024**, 2312894; cJ. Wu, X. Gao, G. Liu, X. Qiu, Q. Xia, X. Wang, W. Zhu, T. He, Y. Zhou, K. Feng, J. Wang, H. Huang, Y. Liu, M. Shao, Z. Kang, X. Zhang, *J. Am. Chem. Soc.* **2024**.

[2] aX. H. Zou, M. C. Tang, Q. Lu, Y. Wang, Z. P. Shao, L. An, *Energy Environ. Sci.* **2024**, *17*, 386-424; bQ. Lu, X. H. Zou, Y. F. Bu, Z. P. Shao, *Energy Storage Mater.* **2023**, *55*, 166-192; cW. Sun, F. Wang, B. Zhang, M. Y. Zhang, V. Küpers, X. Ji, C. Theile, P. Bieker, K. Xu, C. S. Wang, M. Winter, *Science* **2021**, *371*, 46.

[3] aX. H. Zou, Q. Lu, J. Wu, K. E. Zhang, M. C. Tang, B. X. Wu, S. X. She, X. Zhang, Z. P. Shao, L. An, *Adv. Funct. Mater.* **2024**; bQ. Lu, X. H. Zou, Y. F. Bu, Y. Wang, Z. P. Shao, *Energy Storage Mater.* **2024**, *68*, 103341.

[4] aY. He, W. X. Shang, M. Ni, Y. Y. Huang, H. Zhao, P. Tan, *Chem. Eng. J.* **2022**, *427*, 130862; bG. Y. Li, Y. T. Long, Z. Li, S. P. Li, Y. Zheng, B. H. He, M. Zhou, Z. Q. Hu, M. J. Zhou, Z. H. Hou, *ACS Sustainable Chem. Eng.* **2023**, *11*, 8642-8650; cM. Wu, Y. Xu, J. Luo, S. Yang, G. Zhang, L. Du, H. Luo, X. Cui, Y. Yang, S. Sun, *Angew. Chem. Int. Ed.* **2024**, e202410845.

[5] aT. Wang, Z. L. Tian, Z. H. You, Z. Li, H. Cheng, W. Z. Li, Y. H. Yang, Y. G. Zhou, Q. F. Zhong, Y. Q. Lai, *Energy Storage Mater.* **2022**, *45*, 24-32; bZ. X. Zhao, Y. He, W. T. Yu, W. X. Shang, Y. Y. Ma, Z. J. Zhang, P. Tan, *J. Electrochem. Soc.* **2022**, *169*, 100551; cX. H. Zou, Q. Lu, C. E. Wang, S. X. She, K. M. Liao, R. Ran, W. Zhou, L. An, Z. P. Shao, *J. Membr. Sci.* **2023**, *665*, 121112; dM. C. Tang, Q. Liu, Z. L. Yu, X. H. Zou, X. Y. Huo, B. Zhang, L. An, *Small* **2024**, 2403457; eK. E. Zhang, P. T. Sun, Y. L. Huang, M. C. Tang, X. H. Zou, Z. F. Pan, X. Y. Huo, J. Wu, C. C. Lin, Z. T. Sun, Y. Y. Wan, X. Zhang, L. An, *Adv. Funct. Mater.* **2024**, 2405179.

[6] Y. H. Chen, J. J. Xu, P. He, Y. Qiao, S. H. Guo, H. J. Yang, H. S. Zhou, *Sci. Bull.* **2022**, *67*, 2449-2486.

[7] S. Q. Huang, H. Zhang, J. H. Zhuang, M. Y. Zhou, M. Q. Gao, F. F. Zhang, Q. Wang, *Adv. Energy Mater.* **2022**, *12*, 2103622.

[8] aM. B. Poudel, M. P. Balanay, P. C. Lohani, K. Sekar, D. J. Yoo, *Adv. Energy Mater.* **2024**, *14*, 2400347; bR. S. Kumar, P. Mannu, S. Prabhakaran, T. T. T. Nga, Y. Kim, D. Kim, J. L. Chen, C. L. Dong, D. J. Yoo, *Adv. Sci.* **2023**, *10*, 2303525; cM. B. Poudel, S. Vijayapradeep, K. Sekar, J. S. Kim, D. J. Yoo, *J. Mater. Chem. A* **2024**, *12*, 10185-10195; dR. S. Kumar, S. Prabhakaran, S. Ramakrishnan, S. C. Karthikeyan, A. R. Kim, D. Kim, D. J. Yoo, *Small* **2023**, *19*, 2207096.

[9] Z. S. Song, J. Ding, B. Liu, X. R. Liu, X. P. Han, Y. D. Deng, W. B. Hu, C. Zhong, *Adv. Mater.* **2020**, *32*, 1908127.

[10] M. W. Cui, N. G. Ma, H. Lei, Y. F. Liu, W. Ling, S. Chen, J. Q. Wang, H. F. Li, Z. H. Li, J. Fan, Y. Huang, *Angew. Chem. Int. Ed.* **2023**, *62*, e202303845.

[11] S. Y. Zhao, T. Liu, Y. W. Dai, J. Wang, Y. Wang, Z. J. Guo, J. Yu, I. T. Bello, M. Ni, *Appl. Catal. B-Environ.* **2023**, *320*, 121992.

[12] H. C. Zhang, Y. J. Li, Y. S. Zhao, G. H. Li, F. Zhang, *ACS Appl. Mater. Interfaces* **2019**, *11*, 27846-27853.

[13] X. L. Li, M. Li, Z. D. Huang, G. J. Liang, Z. Chen, Q. Yang, Q. Huang, C. Y. Zhi, *Energy Environ. Sci.* **2021**, *14*, 407-413.

[14] aQ. Zhang, Y. L. Ma, Y. Lu, Y. X. Ni, L. Lin, Z. K. Hao, Z. H. Yan, Q. Zhao, J. Chen, *J. Am. Chem. Soc.* **2022**, *144*, 18435-18443; bY. P. Zou, T. T. Liu, Q. J. Du, Y. Y. Li, H. B. Yi, X. Zhou, Z. X. Li, L. J. Gao, L. Zhang, X. Liang, *Nat. Commun.* **2021**, *12*, 170.

[15] aC. G. Wang, X. X. Ji, J. N. Liang, S. S. Zhao, X. X. Zhang, G. M. Qu, W. F. Shao, C. L. Li, G. Zhao, X. J. Xu, H. Q. Li, *Angew. Chem. Int. Ed.* **2024**, *63*, e202403187; bM. X. Ji, J. Di, Y. L. Liu, R. Chen, K. Li, Z. G. Chen, J. X. Xia, H. M. Li, *Appl. Catal. B-Environ.* **2020**, *268*, 118403.

[16] aR. Kushwaha, S. Haldar, P. Shekhar, A. Krishnan, J. Saha, P. Hui, C. P. Vinod, C. Subramaniam, R. Vaidhyanathan, *Adv. Energy Mater.* **2021**, *11*, 2003626; bO. W. Sheng, H. L. Hu, T. F. Liu, Z. J. Ju, G. X. Lu, Y. J. Liu, J. W. Nai, Y. Wang, W. K. Zhang, X. Y. Tao, *Adv. Funct. Mater.* **2022**, *32*, 2111026; cJ. Kang, F. Cintron-Colon, H. Kim, J. Kim, T. Varga, Y. G. Du, O. Qafoku, W. Um, T. G. Levitskaia, *Chem. Eng. J.* **2022**, *430*, 132788.

[17] aQ. Q. Liu, C. F. Xia, C. H. He, W. Guo, Z. P. Wu, Z. Li, Q. Zhao, B. Y. Xia, *Angew. Chem. Int. Ed.* **2022**, *61*, e202210567; bS. P. Wang, Y. W. Zhao, H. M. Lv, X. H. Hu, J. He, C. Y. Zhi, H. F. Li, *Small* **2023**, 2207664.

[18] A. R. Mainar, E. Iruin, L. C. Colmenares, A. Kvasha, I. de Meatza, M. Bengoechea, O. Leonet, I. Boyano, Z. C. Zhang, J. A. Blazquez, *J. Energy Storage* **2018**, *15*, 304-328.

[19] aL. Y. Li, Y. C. A. Tsang, D. W. Xiao, G. Y. Zhu, C. Y. Zhi, Q. Chen, *Nat. Commun.* **2022**, *13*, 2870; bX. C. Chen, Z. Zhou, H. E. Karahan, Q. Shao, L. Wei, Y. Chen, *Small* **2018**, *14*, 1801929; cQ. Lu, X. Zou, Y. Bu, L. An, Y. Wang, Z. Shao, *Next Energy* **2023**, *1*; dA. Li, J. Y. Li, Y. R. He, M. C. Wu, *J. Energy Chem.* **2023**, *83*, 209-228.

[20] aY. He, P. Tan, *Chem-A Eur. J.* **2024**, *30*, e202303477; bY. He, Z. X. Zhao, Y. F. Cui, W. X. Shang, Y. T. Chen, P. Tan, *Energy Storage Mater.* **2023**, *57*, 360-370; cL. Z. Wu, Z. F. Pan, S. Yuan, X. Y. Shi, Y. Liu, F. T. Liu, X. H. Yan, L. An, *Chem. Eng. J.* **2024**, *488*, 151000.

## Entry for the Table of Contents

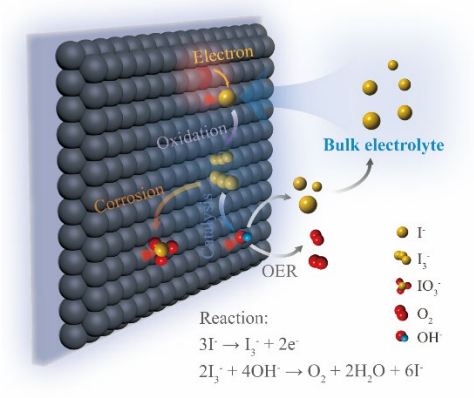


We apply acetylene black catalysts to achieve an $I_3^-$-mediated Zn-air battery by using $ZnI_2$ additives that provide $I_3^-$ during the electrochemically charging process to chemically react with $OH^-$ to generate oxygen and further revert to $I^-$, thus obtaining a stable electrochemical system.